HHS Public Access

Author manuscript

*Anal Bioanal Chem*. Author manuscript; available in PMC 2018 October 01.

Published in final edited form as:

*Anal Bioanal Chem*. 2017 October ; 409(25): 5955–5964. doi:10.1007/s00216-017-0514-4.

# An LC-MS Chemical Derivatization Method for the Measurement of Five Different One-carbon States of Cellular Tetrahydrofolate

**Li Chen**, **Gregory S. Ducker**, **Wenyun Lu**, **Xin Teng**, and **Joshua D. Rabinowitz***

Lewis-Sigler Institute for Integrative Genomics and Department of Chemistry, Princeton University, Princeton, New Jersey 08544, United States

## Abstract

The cofactor tetrahydrofolate (THF) is used to reduce, oxidize and transfer one-carbon (1C) units required for the synthesis of nucleotides, glycine, and methionine. Measurement of intracellular THF species is complicated by their chemical instability, signal dilution caused by variable polyglutamation and the potential for interconversion among these species. Here we describe a method using negative mode liquid chromatography-mass spectrometry (LC-MS) to measure intracellular folate species from mammalian cells. Application of this method with isotope-labeled substrates revealed abiotic interconversion of THF and methylene-THF, which renders their separate quantitation particularly challenging. Chemical reduction of methylene-THF using deuterated sodium cyanoborohydride traps methylene-THF, which is unstable, as deuterated 5-methyl-THF, which is stable. Together with proper sample handling and LC-MS, this enables effective measurements of five active folate pools (THF, 5-methyl-THF, methylene-THF, methenyl-THF/10-formyl-THF, and 5-formyl-THF) representing the biologically important 1C oxidation states of THF in mammalian cells.

## Graphic Abstract

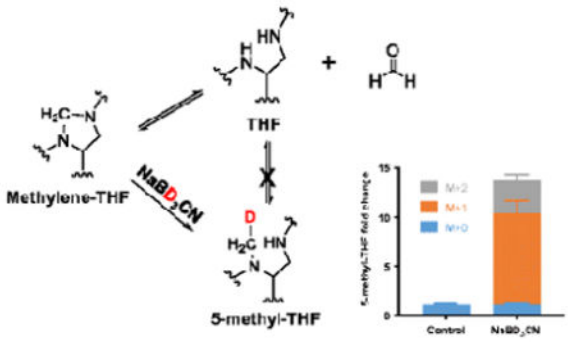


### Keywords

Folate; Chemical derivatization; Methylene-THF; LC-MS; Interconversion; One-carbon metabolism

*Corresponding author: Joshr@princeton.edu.

**Compliance with ethical standards**

**Conflict of interest** The authors declare that they have no conflict of interest.

## Introduction

Folate is an essential dietary vitamin commonly measured in food, plants, serum, urine and tissues (1–7). Folates are a family of pteroylglutamate species in various oxidation states. The most reduced form, and biologically active species, tetrahydrofolate (THF) (8), mediates one-carbon (1C) metabolism which is required for the synthesis of thymidine, purines, methionine, and glycine. These 1C metabolic reactions are essential for fetal growth (9), proliferation of adult tissues, and cancer progression (10, 11). Recent work has uncovered roles for folate metabolism in redox homeostasis and methylation regulation (12, 13). Inhibitors of these processes (antifolates) are commonly used as immunosuppressive and anticancer agents.

Chemically, 1C units are carried on the reduced pteridine ring of THF (Figure 1). This ring can accommodate a 1C group in various oxidation states through different bonding between the 1C unit and the ring's 5-position and exocyclic 10-position nitrogen atoms. The most reduced one-carbon species, 5-methyl-THF, is used in the synthesis of methionine; the intermediate oxidation state of 5,10-methylene-THF is used for thymidine synthesis and for serine-glycine interconversion; and the most oxidized 1C species, 10-formyl-THF, is used in the synthesis of purines (Figure 1). Methenyl-THF is an intermediate between methylene-THF and 10-formyl-THF, and is at the same oxidation state as 10-formyl-THF. A positional isomer of 10-formyl-THF, 5-formyl-THF (folinic acid or leucovorin), serves as a stable formyl storage molecule. It is commonly used clinically to mitigate the side effects of antifolates through intracellular interconversion to methenyl-THF, but is not a fundamental biosynthetic precursor by itself (14). In summary, there exist five 1C bound states of THF (methyl, methylene, methenyl, 10-formyl, 5-formyl) representing three oxidation states of the 1C unit.

The measurement of the set of active folate species from cell or tissue samples is complicated by three main factors: chemical susceptibility to oxidation, the variable extent of THF polyglutamation, and the potential for interconversion among these species. Similar issue arise also in analysis of folates in foods (15–18). By comparison, measurement of serum folates is simpler because oxidative degradation can be readily addressed by ascorbic acid, extracellular folates are not polyglutamated and the chemical forms are largely limited to folate and 5-methyl-THF (5), which do not interconvert. Consequently, while the chemistry of folate interconversions has been established (19), it is not commonly addressed in bioanalytical methods that have been mainly developed for serum samples (5).

Folates from intracellular samples are polyglutamated to retain them inside the cell and to enhance enzyme binding, a process that creates a distribution of molecular formulas and thus masses for every pteridine form. Methods for measuring the full scope of different polyglutamated THF species by LC-MS have been reported in bacteria (20). In mammalian cells, however, the abundance of these species is lower and the diversity of polyglutamated species greater (21). Accordingly, measurement relies on polyglutamate removal, condensing polyglutamated forms into a single monoglutamate pool. This is typically

accomplished with rat serum (18, 22), which has substantial glutamate carboxypeptidase activity (23).

In developing an LC-MS method to analyze folates from cells treated with isotope tracers, we observed systematic discrepancies between the labeling of different folate species, and between certain folate species and their downstream metabolic products. This reflects post-lysis chemical interconversions that affect the measurements of the individual folate forms. To overcome these interconversion problems, we denatured enzyme activity in the lysates by brief heat treatment. In addition, we developed a derivatization technique using sodium cyanoborodeuteride ($NaBD_3CN$) reduction to convert methylene-THF into deuterium ($^2H$)-labeled 5-methyl-THF. This technique enables accurate measurement of the THF and methylene-THF pools. Together, our optimized protocol allows for the accurate determination of free cellular THF and each of the different 1C-bound THF pools encompassing the biologically relevant oxidation states.

## Material and methods

### 1) Chemicals and solvents

Standards of all folate species were obtained from Schircks Laboratories except 10-formyl-THF, which was not commercially available and was prepared according to previous literature (24). Stable isotope compounds [3-$^{13}C$]serine, [$^{13}C$,$^2H$]sodium formate, [uniform (U)-$^2H$]MeOH, [U-$^2H$]formaldehyde were obtained from Cambridge Isotope Laboratories. Rat serum, activated charcoal, $NaBH_3CN$ and $NaBD_3CN$ were obtained from Sigma. HPLC-grade water, methanol and acetonitrile (Optima) were obtained from ThermoFisher Scientific.

### 2) Cell culture

HEK293T cells (ATCC, CRL-11268) were grown in DMEM (Cellgro, 10-017) without pyruvate and supplemented with 10% FBS (Sigma) in an incubator with 5% $CO_2$ and ambient oxygen at 37°C. Cell volume was measured by packed cell volume tubes (MIDSCI). For isotope labeling experiments, cells were plated into 6 cm plates, grown for 1 day before switching to DMEM medium with tracers as indicated ([3-$^{13}C$]-serine in place of the normal serine in the medium, or [$^{13}C$,$^2H$]-sodium formate added to the medium) supplemented with 10% dialyzed FBS (Sigma). Cells were incubated in the isotopic labeling medium for 24 h and were switched to fresh labeling medium 2 h before extraction. Cells were collected at 60% to 90% confluency.

### 3) Metabolite extraction and LC-MS analysis

For general small molecule metabolite extraction (not folate species), adherent cells were washed rapidly with PBS 3 times at room temperature (washing was required because the focus of the analysis was intracellular amino acid labeling) before adding 80:20 $H_2O$:MeOH at −80°C. Supernatants were collected, dried down under $N_2$ flow, resuspended in HPLC water, and kept at 4°C in an autosampler. Samples were analyzed by a stand-alone orbitrap mass spectrometer (ThermoFisher Exactive) operating in negative ion mode and coupled to reverse-phase ion-pairing chromatography method via electrospray ionization as described

previously (25). Briefly, liquid chromatography separation was achieved on a Synergy Hydro-RP column (100 mm×2 mm, 2.5μm particle size, Phenomenex) with a flow rate of 200 μL/min. Solvent A was 97:3 $H_2O$:MeOH with 10 mM tributylamine and 15 mM acetic acid; solvent B was methanol. The gradient was 0 min, 0% B; 2.5 min, 0% B; 5 min, 20% B; 7.5 min, 20% B; 13 min, 55% B; 15.5 min, 95% B; 18.5 min, 95% B; 19 min, 0% B; 25 min, 0% B. For mass spectrometry, an electrospray ionization interface was used to direct column eluent to an Exactive Orbitrap high resolution high accuracy mass spectrometer operating in negative ion mode, with a resolution of 100,000 at m/z 200. Scan window is m/z = 75 to 1000. AGC (automatic gain control) targets $3\times10^6$. Maximum injection time is 250 ms. Data were analyzed using the MAVEN software package (26, 27). Data from labelling experiments were adjusted for natural $^{13}C$, $^{15}N$, $^{2}H$ and $^{18}O$ abundance and impurity of labeled substrate using in-house correction code running in R (28). LC-MS method for folates was the same, except for a small modification of the LC gradient (see below). While the high-resolution full scan capabilities of the Orbitrap are convenient for labeling studies, similar results can be obtained using other types of mass spectrometry, including full scan analysis on a time-of-flight instrument or, with pre-programming of the relevant ion masses and fragmentation reactions, targeted analysis on a triple quadruple instrument (5, 29), with the latter holding the potential for superior for sensitivity and precision when measuring only a few analytes.

### 4) Folate extraction and LC-MS analysis

Folates were extracted from cultured cells in 6 cm plates by aspirating media and immediately adding 1 mL ice cold 50:50 $H_2O$:MeOH containing 25 mM sodium ascorbate and 25 mM $NH_4OAc$ at pH 7. Plates were kept on ice and cells were scraped and the resulting mixture of cells and solvent transferred to 1.5 mL centrifuge tubes after 30 min. Tubes were heated to 60 °C for 5 min to fully denature proteins, and precipitates were removed by centrifugation at 16000 × g for 5 min at 4 °C. To cleave glutamate tails, supernatants were dried under $N_2$ flow and resuspended in 450 μL potassium phosphate buffer (50 mM with 30 mM ascorbic acid and 0.5% 2-mercaptoethanol at pH 7). 25 μL rat serum pretreated with activated charcoal to remove endogenous folate (3) was added to the samples before incubating at 37 °C for 2 h. We measured folate content in the serum before and after activated charcoal treatment, and the charcoal-treatment depleted rat serum folates to undetectable levels. To clean up samples before LC-MS, Bond Elut-PH SPE columns (Agilent) were conditioned with 1 mL MeOH and then with 1 mL wash buffer (30 mM ascorbic acid in 25 mM $NH_4OAc$ buffer at pH 4.0). After adjusting the samples to pH 4 with 7 μL of 40% formic acid solution at 4°C, the samples were loaded onto the conditioned SPE columns, washed with 1 mL wash buffer and subsequently eluted with 400 μL elution buffer (50:50 $H_2O$:MeOH containing 0.5% 2-mercaptoethanol and 25 mM $NH_4OAc$ at pH 7). The eluate was dried down under $N_2$ flow, resuspended into HPLC water, centrifuged to remove possible precipitate, kept at 4°C in an autosampler and analyzed by LC-MS within 12 h to minimize degradation. Sample analysis was the same as described above with modification in the LC gradient, 0 min, 0% B; 2.5 min, 0% B; 5 min, 50% B; 13 min, 95% B; 14 min, 0% B; 20 min, 0% B. Mass spectrometry setup was the same except the scan window was m/z = 400 to 1000. In the case of $NaBH_3CN$ or $NaBD_3CN$ reduction, before cell extraction, 1 M $NaBH_3CN$ or $NaBD_3CN$ stock solution was added to 50:50 $H_2O$:acetonitrile extraction

buffer containing 25 mM sodium ascorbate and 25 mM HEPES (4-(2-hydroxyethyl)piperazine-1-ethanesulfonic acid) at pH 7 to a final concentration of 25 mM. Acetonitrile was used in place of methanol for extraction prior to derivatization, to avoid potential impact of formaldehyde, which is an impurity in methanol. The subsequent procedure was identical except 4 μL of 40% formic acid was added to adjust pH to 4 before SPE purification. For quantification of total pool size of THF species, 4 pmol of different THF species standards were spiked in to cell extracts before heat treatment.

## Results and discussion

### 1. LC-MS-based quantification of THF species in cultured human cells

The concentration of cellular THF species is in the nM to μM range (2, 3), and these species exist in multiple polyglutamated forms (30). This polyglutamation creates analytical challenges by decreasing the signal intensity for each functional THF species in mass spectrometry. To combat this, we used rat serum treatment to cleave the polyglutamate chains from folate species and condense them into monoglutamate forms. THF species from treated samples were then purified and concentrated by solid phase extraction before LC-MS analysis (Figure 2a). We employed reverse-phase chromatography on a C18 column coupled to an Orbitrap mass spectrometer operating in negative ion mode. We confirmed the peak identify and detection limits for all folate species using our LC-MS method by purified standards (Table 1). We then applied the above approach to analyze THF species from cultured mammalian cells. From 5 μL (packed cell volume, PCV) of HEK293T cells which roughly corresponds to $3\times10^6$ cells, we could isolate and detect distinct peaks for THF, 5-methyl-THF, methylene-THF, and methenyl-THF. For formyl-THF (m/z= 472.158), two peaks were observed, corresponding to 10-formyl-THF (RT = 9.56 min) and 5-formyl-THF (RT = 9.72 min) (Figure 2b). Thus, our protocol appeared to effectively quantify the major THF species in cultured mammalian cells.

### 2. Residual enzymatic activity in lysates converts 5-formyl-THF to methenyl-THF

10-formyl-THF provides a formyl unit in biosynthetic reactions and can also be oxidized or reduced to other 1C forms, while 5-formyl-THF is a storage molecule which contributes to biosynthetic 1C reactions only after being converted to methenyl-THF by an ATP-consuming enzyme (14). Therefore, these two formyl-THF species have distinct biological roles. In addition to these enzyme catalyzed transformations, both 10- and 5-formyl-THF can interconvert with methenyl-THF via spontaneous water loss (Figure 3a).

Upon mixing methenyl-THF standard in water at 4°C, 10-formyl-THF was observed. In deuterated water, hydrogen-deuterium (H-D) exchange between methenyl-THF and 10-formyl-THF occurred with a half-life of ~4 h at 4°C. The more chemically stable 5-formyl-THF did not undergo such H-D exchange (Figure 3b). Cellular 10-formyl-THF can be carbon and deuterium labeled by the incorporation of exogenous [$^{13}$C, $^{2}$H]-formate by the formyl ligase activity of MTHFD1 (31, 32). This should result in M+2 10-formyl-THF, and M+2 and M+4 ADP (which contains two 10-formyl THF 1C units). Indeed, upon feeding [$^{13}$C, $^{2}$H]-formate, ADP was mainly M+2 and M+4 labeled, with only a minimal M+1 and M+3 fractions, indicating limited deuteron exchange in cells. In contrast, we only observed

M+1 10-formyl-THF suggesting that a deuteron had been lost after cell lysis (Figure 3c). This result is consistent with the known interconversion between 10-formyl-THF and methenyl-THF (33). Together, these data show that the formyl unit on cellular 10-formyl-THF is used before it can exchange with solvent, but that abiotic exchange reactions preclude accurate measurement of 10-formyl-THF deuterium labeling or distinct quantitation of 10-formyl-THF and methenyl-THF.

We next examined whether 5-formyl-THF itself was stable during our procedure. Unexpectedly, when we spiked 4 pmol 5-formyl-THF standard into the supernatant of HEK293T cell lysate, increased methenyl-THF and 10-formyl-THF signals were observed suggesting conversion of 5-formyl-THF into methenyl- and 10-formyl-THF. This conversion was not observed with standard alone (Figure 3d), implicating residual enzymatic activity in lysate as the cause. Consistent with this hypothesis, heating the cell extract at 60°C for 5 min before spiking in 5-formyl-THF standard abolished the conversion of 5-formyl-THF to methenyl-THF. With sample heating to eliminate residual enzymatic activity, 5-formyl-THF can be measured separately from 10-formyl-THF and methenyl-THF.

### 3. Methylene-THF's 1C unit exchanges with free formaldehyde

Methylene-THF dissociates into THF and formaldehyde in solution (Figure 4a). Previous literature reported either the total pool of methylene-THF and THF, or fully converted methylene-THF into THF or methyl-THF, and calculated the individual pools by comparing converted and non-converted samples (34, 35). However, the possibility for THF to condense with formaldehyde to form methylene-THF abiotically has not been addressed. Using stable isotope labeling, we found that the trace formaldehyde in the methanol used in sample preparation and chromatography can condense with THF to form methylene-THF.

In HEK293T cells, cytosolic methylene-THF is produced from 10-formyl-THF (36). In cells fed with [$^{13}$C, $^{2}$H]-formate, methylene-THF and its downstream products methyl-THF and dTTP were expected to be M+2 labeled. Indeed, the detected 5-methyl-THF and dTTP were mostly M+2 labeled. However, methylene-THF was not labeled, indicating the methylene unit is exchanging during or after extraction (Figure 4b).

Similar results were obtained in cells fed [3-$^{13}$C]-serine. Steady state labeling with [3-$^{13}$C]-serine resulted in M+1 labeling of intracellular serine (~ 60%) and did not label THF itself (which lacks a 1C unit and therefore should not be labeled). The observed $^{13}$C labeling of dTTP and methyl-THF matched that of serine, confirming that folates were being labeled intracellularly. However, $^{13}$C enrichment was not observed in methylene-THF, which provides the 1C unit in dTTP (Figure 4c). Thus, the methylene-THF 1C unit is subject to abiotic exchange with organic solvent, but intracellular reactions happen much faster than abiotic exchange.

To explore the abiotic 1C-unit exchange on methylene-THF, purified methylene-THF standard was dissolved in 50:50 $^{2}$H-methanol:$H_2O$ containing 25 mM $NH_4OAc$ and 25 mM ascorbate. The standard became M+2 labeled in a time-dependent manner (Figure 4d). When $^{2}$H-formaldehyde was added to unlabeled methanol:$H_2O$, the M+2 fraction of methylene-THF standard increased in a formaldehyde concentration-dependent manner

(Figure 4e). Thus, methylene-THF not only dissociates to THF and formaldehyde, but, even at low formaldehyde concentrations, can be formed by condensation of THF and formaldehyde. A typical contamination of 0.5 ppm formaldehyde (13 μM) in HPLC grade methanol (37) is more than 100-fold in excess of the THF concentration during a folate extraction from mammalian cells. In summary, methylene-THF is in abiotic exchange with THF and formaldehyde contaminant present in methanol.

### 4. Quantification of methylene-THF with $NaBD_3CN$ reduction

To circumvent the abiotic interconversion of THF and methylene-THF, we employed a chemical strategy to reduce methylene-THF to 5-methyl-THF during the cellular extraction. Initially, we tried adding 25mM $NaBH_4$ into the extraction solvent at pH 10 to reduce methylene-THF (35), and observed effective reduction of methylene-THF standard. However, when we spiked standards of methylene-THF into the cell extract and performed the reduction, we only observed 50% conversion (see Electronic Supplementary Material (ESM) Fig. S1). We hypothesized that this reflected consumption of the reducing agent by reaction with other cell lysate components. Accordingly, rather than moving to a stronger reducing agent, we elected to test the less reactive $NaBH_3CN$, in the hopes that it might more specifically react with the methylene-THF (Figure 5a). To further increase specificity, we also lowered the pH to 7.0. Under these conditions, the reaction went to completion within 5 minutes at 37 °C. To validate the effectiveness of the reduction approach, we performed the reaction on [3-$^{13}$C]-serine labeled cells, and observed an increase in both labeled and unlabeled 5-methyl-THF (Figure 5b), indicating that we were effectively capturing biologically active methylene-THF. Thus the reduction reaction was rapid relative to the undesired abiotic interconversion, enabling methylene-THF to be accurately distinguished from THF despite their inherent chemical instability.

To discriminate between natural and synthetically generated 5-methyl-THF, we used $^2$H-labeled reducing agent. $NaBD_3CN$ reduction results in multiple isotopically labeled forms of 5-methyl-THF (Figure 5c). Using standards, we determined that methylene-THF was reduced primarily to M+1 5-methyl-THF, whereas methenyl-THF and dihydrofolate (in the presence of trace formaldehyde) were reduced to M+2 5-methyl-THF (Figure 5d). After correction for natural isotopic abundances, we assigned the respective M+0, M+1, M+2 signals to endogenous 5-methyl-THF, methylene-THF reduction, and reduction of more oxidized folate species including methenyl-THF and dihydrofolate. The M+0 and M+1 signal thus enable resolved quantitation of cellular THF and methylene-THF.

### 5. THF species pool sizes in HEK293T cells and effect of methotrexate

With our refined measurement techniques, we report the absolute concentrations in mammalian cells for five folate pools representing the three most important biological 1C unit oxidation states. These are: THF, methylene-THF, methenyl-THF/10-formyl-THF, 5-formyl-THF, and 5-methyl-THF. We quantified the absolute concentrations of THF species corresponding to these five pools in growing HEK293T cells by spiking commercially available standards into cell lysates (Table 2, ESM Fig. S2). Specific measurement of methylene-THF pool was achieved by applying the $NaBD_3CN$ reduction method. Consistent with prior literature using microbiological (38, 39) and radioactive assays(40, 41), the total

pool of THF species was ~ 4 μM, and was relatively evenly spread between THF, methylene-THF, and the combined pool of methenyl-THF and 10-formyl-THF, with 5-formyl-THF and 5-methyl-THF lower in abundance. We observed a lower concentration of 5-formyl-THF in HEK293T cells than reported in either K562 or MCF7 cells (39, 40).

We also evaluated the changes in folate pool sizes induced by the common antifolate drug methotrexate. Methotrexate treatment (1 μM, 2 h) resulted in a 30-fold increase of DHF and 3- to 12-fold decreases in different THF species (Figure 6), consistent with methotrexate inhibiting dihydrofolate reductase, its canonical target (42, 43).

## Conclusion

Isotope tracers combined with LC-MS analysis are powerful tools for studying cellular metabolism. We developed an approach to measure both the concentrations and isotopic labeling of various THF species in mammalian cells. The use of isotopic tracers uncovered key abiotic interconversions among THF species that occur in biological samples after lysis (19). Such interconversions, which have likely impacted many prior folate analyses, allow only three different mixed 1C pools to be independently measured using standard LC-MS methods: THF/methylene-THF, methenyl-THF/formyl-THF, and methyl-THF. Through a $NaBD_3CN$ reduction strategy, we demonstrate a method to discriminate methylene-THF from THF and thus enable the accurate measurement of both species. Furthermore, by adding a brief heating step to eliminate residual enzymatic activity, we can differentiate the formyl-THF pool into 5-formyl-THF and combined methenyl-THF and 10-formyl-THF. Accordingly, we believe the best approach for folate measurement from mammalian cells involves the generation of two extracts, one being heated at 60°C for 5 minutes to eliminate residual enzymatic activity, and the other utilizing $NaBD_3CN$ in the extraction solvent. Common workup and LC-MS analysis of both of these extracts enables quantification and isotope tracing studies of five biologically important THF pools, encompassing all major biologically relevant 1C oxidation states. These methods should accelerate quantitative understanding of 1C metabolism, a topic of great current interest and enduring biomedical importance (10, 11, 44, 45).

## Supplementary Material

Refer to Web version on PubMed Central for supplementary material.

## Acknowledgments

This research was supported in part by funding to J.D.R. from the U.S. National Institutes of Health (NIH) (R01CA16359-01A1) and Stand Up to Cancer (SU2C-AACR-DT0509). G.S.D. was supported by a postdoctoral fellowship (PF-15-190-01-TBE) from the American Cancer Society. W.L. was supported by NIH (CA211437).

## References

1. Pai YJ, Leung KY, Savery D, Hutchin T, Prunty H, Heales S, et al. Glycine decarboxylase deficiency causes neural tube defects and features of non-ketotic hyperglycinemia in mice. Nat Commun. 2015; 6:6388. [PubMed: 25736695]

2. Taflin H, Wettergren Y, Odin E, Derwinger K. Folate levels measured by LC-MS/MS in patients with colorectal cancer treated with different leucovorin dosages. Cancer Chemother Pharmacol. 2014; 74(6):1167–74. [PubMed: 25238909]

3. Odin E, Wettergren Y, Carlsson G, Gustavsson B. Determination of reduced folates in tumor and adjacent mucosa of colorectal cancer patients using LC-MS/MS. Biomedical chromatography : BMC. 2013; 27(4):487–95. [PubMed: 22991184]

4. Niesser M, Harder U, Koletzko B, Peissner W. Quantification of urinary folate catabolites using liquid chromatography-tandem mass spectrometry. J Chromatogr B Analyt Technol Biomed Life Sci. 2013; 929:116–24.

5. Fazili Z, Whitehead RD Jr, Paladugula N, Pfeiffer CM. A high-throughput LC-MS/MS method suitable for population biomonitoring measures five serum folate vitamers and one oxidation product. Anal Bioanal Chem. 2013; 405(13):4549–60. [PubMed: 23462981]

6. Camara JE, Lowenthal MS, Phinney KW. Determination of fortified and endogenous folates in food-based Standard Reference Materials by liquid chromatography-tandem mass spectrometry. Anal Bioanal Chem. 2013; 405(13):4561–8. [PubMed: 23354578]

7. Buttner BE, Ohrvik VE, Kohler P, Witthoft CM, Rychlik M. Quantification of isotope-labeled and unlabeled folates and folate catabolites in urine samples by stable isotope dilution assay. International journal for vitamin and nutrition research Internationale Zeitschrift fur Vitamin- und Ernahrungsforschung Journal international de vitaminologie et de nutrition. 2013; 83(2):112–21. [PubMed: 24491884]

8. Wright AJ, Dainty JR, Finglas PM. Folic acid metabolism in human subjects revisited: potential implications for proposed mandatory folic acid fortification in the UK. Br J Nutr. 2007; 98(4):667–75. [PubMed: 17617936]

9. Kalhan SC, Marczewski SE. Methionine, homocysteine, one carbon metabolism and fetal growth. Rev Endocr Metab Disord. 2012; 13(2):109–19. [PubMed: 22418620]

10. Locasale JW. Serine, glycine and one-carbon units: cancer metabolism in full circle. Nature reviews Cancer. 2013; 13(8):572–83. [PubMed: 23822983]

11. Ducker GS, Rabinowitz JD. One-Carbon Metabolism in Health and Disease. Cell Metab. 2017; 25(1):27–42. [PubMed: 27641100]

12. Anderson OS, Sant KE, Dolinoy DC. Nutrition and epigenetics: an interplay of dietary methyl donors, one-carbon metabolism and DNA methylation. J Nutr Biochem. 2012; 23(8):853–9. [PubMed: 22749138]

13. Fan J, Ye JB, Kamphorst JJ, Shlomi T, Thompson CB, Rabinowitz JD. Quantitative flux analysis reveals folate-dependent NADPH production. Nature. 2014; 510(7504):298. [PubMed: 24805240]

14. Stover P, Schirch V. The metabolic role of leucovorin. Trends in biochemical sciences. 1993; 18(3): 102–6. [PubMed: 8480361]

15. O'Broin JD, Temperley IJ, Brown JP, Scott JM. Nutritional stability of various naturally occurring monoglutamate derivatives of folic acid. Am J Clin Nutr. 1975; 28(5):438–44. [PubMed: 236647]

16. Lu W, Kwon YK, Rabinowitz JD. Isotope ratio-based profiling of microbial folates. J Am Soc Mass Spectrom. 2007; 18(5):898–909. [PubMed: 17360194]

17. Saini RK, Nile SH, Keum YS. Folates: Chemistry, analysis, occurrence, biofortification and bioavailability. Food Res Int. 2016; 89(Pt 1):1–13. [PubMed: 28460896]

18. Quinlivan EP, Hanson AD, Gregory JF. The analysis of folate and its metabolic precursors in biological samples. Anal Biochem. 2006; 348(2):163–84. [PubMed: 16266679]

19. Jagerstad M, Jastrebova J. 5,10-Methylene-tetrahydrofolate dissociates into tetrahydrofolate and formaldehyde at physiological pH and acidic pH, typical conditions used during sample extraction and LC-MS/MS analysis of biological samples. Biomed Chromatogr. 2014; 28(7):1041–2. [PubMed: 24752933]

20. Kwon YK, Lu W, Melamud E, Khanam N, Bognar A, Rabinowitz JD. A domino effect in antifolate drug action in Escherichia coli. Nat Chem Biol. 2008; 4(10):602–8. [PubMed: 18724364]

21. Lin BF, Huang RF, Shane B. Regulation of folate and one-carbon metabolism in mammalian cells. III. Role of mitochondrial folylpoly-gamma-glutamate synthetase. J Biol Chem. 1993; 268(29): 21674–9. [PubMed: 8408020]

22. Chandra-Hioe MV, Bucknall MP, Arcot J. Folate analysis in foods by UPLC-MS/MS: development and validation of a novel, high throughput quantitative assay; folate levels determined in Australian fortified breads. Anal Bioanal Chem. 2011; 401(3):1035–42. [PubMed: 21667347]
23. Doherty RF, Beecher GR. A method for the analysis of natural and synthetic folate in foods. J Agric Food Chem. 2003; 51(2):354–61. [PubMed: 12517095]
24. Stover P, Schirch V. Synthesis of (6S)-5-formyltetrahydropteroyl-polyglutamates and interconversion to other reduced pteroylpolyglutamate derivatives. Analytical biochemistry. 1992; 202(1):82–8. [PubMed: 1621989]
25. Lu W, Clasquin MF, Melamud E, Amador-Noguez D, Caudy AA, Rabinowitz JD. Metabolomic analysis via reversed-phase ion-pairing liquid chromatography coupled to a stand alone orbitrap mass spectrometer. Anal Chem. 2010; 82(8):3212–21. [PubMed: 20349993]
26. Melamud E, Vastag L, Rabinowitz JD. Metabolomic analysis and visualization engine for LC-MS data. Anal Chem. 2010; 82(23):9818–26. [PubMed: 21049934]
27. Clasquin MF, Melamud E, Rabinowitz JD. LC-MS data processing with MAVEN: a metabolomic analysis and visualization engine. Curr Protoc Bioinformatics. 2012; Chapter 14(Unit14):1.
28. Su X, Lu W, Rabinowitz JD. Metabolite Spectral Accuracy on Orbitraps. Anal Chem. 2017; 89(11):5940–8. [PubMed: 28471646]
29. De Brouwer V, Zhang GF, Storozhenko S, Straeten DV, Lambert WE. pH stability of individual folates during critical sample preparation steps in prevision of the analysis of plant folates. Phytochem Anal. 2007; 18(6):496–508. [PubMed: 17624887]
30. Lawrence SA, Titus SA, Ferguson J, Heineman AL, Taylor SM, Moran RG. Mammalian mitochondrial and cytosolic folylpolyglutamate synthetase maintain the subcellular compartmentalization of folates. J Biol Chem. 2014; 289(42):29386–96. [PubMed: 25164808]
31. Barlowe CK, Appling DR. In vitro evidence for the involvement of mitochondrial folate metabolism in the supply of cytoplasmic one-carbon units. BioFactors. 1988; 1(2):171–6. [PubMed: 2475123]
32. MacFarlane AJ, Perry CA, Girnary HH, Gao D, Allen RH, Stabler SP, et al. Mthfd1 is an essential gene in mice and alters biomarkers of impaired one-carbon metabolism. J Biol Chem. 2009; 284(3):1533–9. [PubMed: 19033438]
33. Stover P, Schirch V. Evidence for the accumulation of a stable intermediate in the nonenzymatic hydrolysis of 5,10-methenyltetrahydropteroylglutamate to 5-formyltetrahydropteroylglutamate. Biochemistry. 1992; 31(7):2148–55. [PubMed: 1536855]
34. Wilson SD, Horne DW. High-performance liquid chromatographic determination of the distribution of naturally occurring folic acid derivatives in rat liver. Anal Biochem. 1984; 142(2): 529–35. [PubMed: 6442107]
35. Horne DW. High-performance liquid chromatographic measurement of 5,10-methylenetetrahydrofolate in liver. Anal Biochem. 2001; 297(2):154–9. [PubMed: 11673882]
36. Ducker GS, Chen L, Morscher RJ, Ghergurovich JM, Esposito M, Teng X, et al. Reversal of Cytosolic One-Carbon Flux Compensates for Loss of the Mitochondrial Folate Pathway. Cell Metab. 2016; 23(6):1140–53. [PubMed: 27211901]
37. Zhong Q, Stowers S, Segraves NL, Ngim KK, Zhang K, Bostick T, et al. Degradation of a pharmaceutical in HPLC grade methanol containing trace level formaldehyde. Pharm Dev Technol. 2013; 18(4):877–82. [PubMed: 22686350]
38. Stempak JM, Sohn KJ, Chiang EP, Shane B, Kim YI. Cell and stage of transformation-specific effects of folate deficiency on methionine cycle intermediates and DNA methylation in an in vitro model. Carcinogenesis. 2005; 26(5):981–90. [PubMed: 15695236]
39. Watkins D, Cooper BA. A critical intracellular concentration of fully reduced non-methylated folate polyglutamates prevents macrocytosis and diminished growth rate of human cell line K562 in culture. Biochem J. 1983; 214(2):465–70. [PubMed: 6577860]
40. Allegra CJ, Fine RL, Drake JC, Chabner BA. The effect of methotrexate on intracellular folate pools in human MCF-7 breast cancer cells. Evidence for direct inhibition of purine synthesis. J Biol Chem. 1986; 261(14):6478–85. [PubMed: 3700401]
41. Fujii K, Nagasaki T, Huennekens FM. Accumulation of 5-methyltetrahydrofolate in cobalamin-deficient L1210 mouse leukemia cells. J Biol Chem. 1982; 257(5):2144–6. [PubMed: 7061412]

42. Huennekens FM. The methotrexate story: a paradigm for development of cancer chemotherapeutic agents. Adv Enzyme Regul. 1994; 34:397–419. [PubMed: 7942284]

43. Mikkelsen TS, Thorn CF, Yang JJ, Ulrich CM, French D, Zaza G, et al. PharmGKB summary: methotrexate pathway. Pharmacogenet Genomics. 2011; 21(10):679–86. [PubMed: 21317831]

44. Amelio I, Cutruzzola F, Antonov A, Agostini M, Melino G. Serine and glycine metabolism in cancer. Trends Biochem Sci. 2014; 39(4):191–8. [PubMed: 24657017]

45. Labuschagne CF, van den Broek NJ, Mackay GM, Vousden KH, Maddocks OD. Serine, but not glycine, supports one-carbon metabolism and proliferation of cancer cells. Cell reports. 2014; 7(4): 1248–58. [PubMed: 24813884]

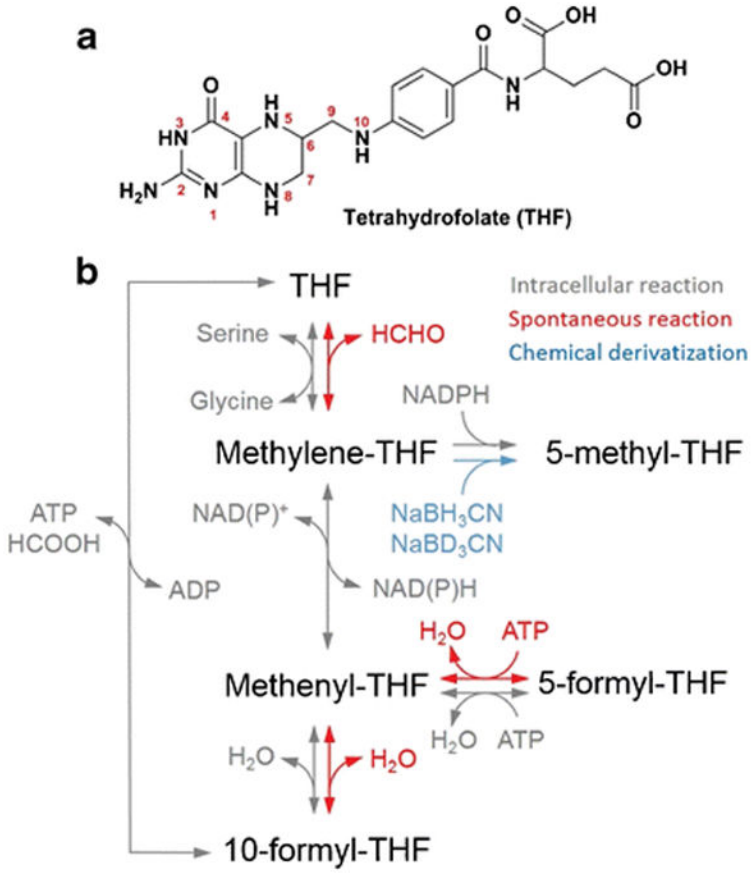


**Figure 1. Tetrahydrofolate (THF) structure and interconversion**

(a) Structure of tetrahydrofolate.

(b) Scheme of intracellular reactions, spontaneous reactions and chemical derivatization of THF species.

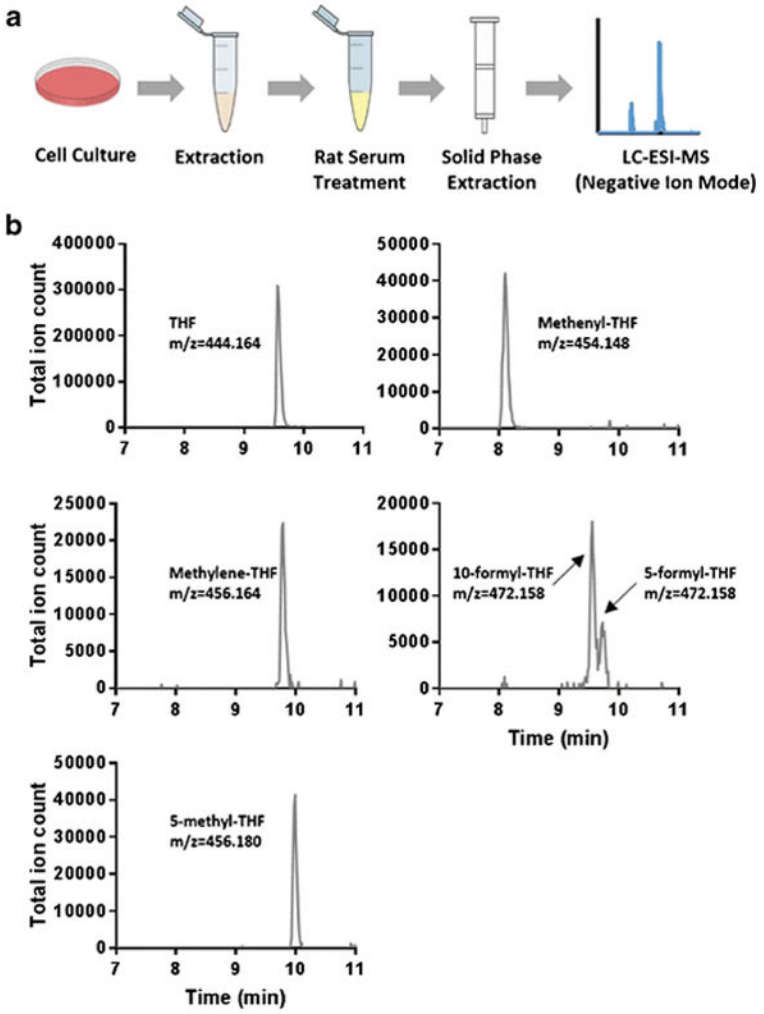


**Figure 2. LC-MS measurement of THF species from cultured cells**

(a) Schematic of analytical workflow.

(b) Extracted ion chromatograms (indicated exact mass ± 10 ppm) of THF, methylene-THF, methenyl-THF, 5/10-formyl-THF and 5-methyl-THF.

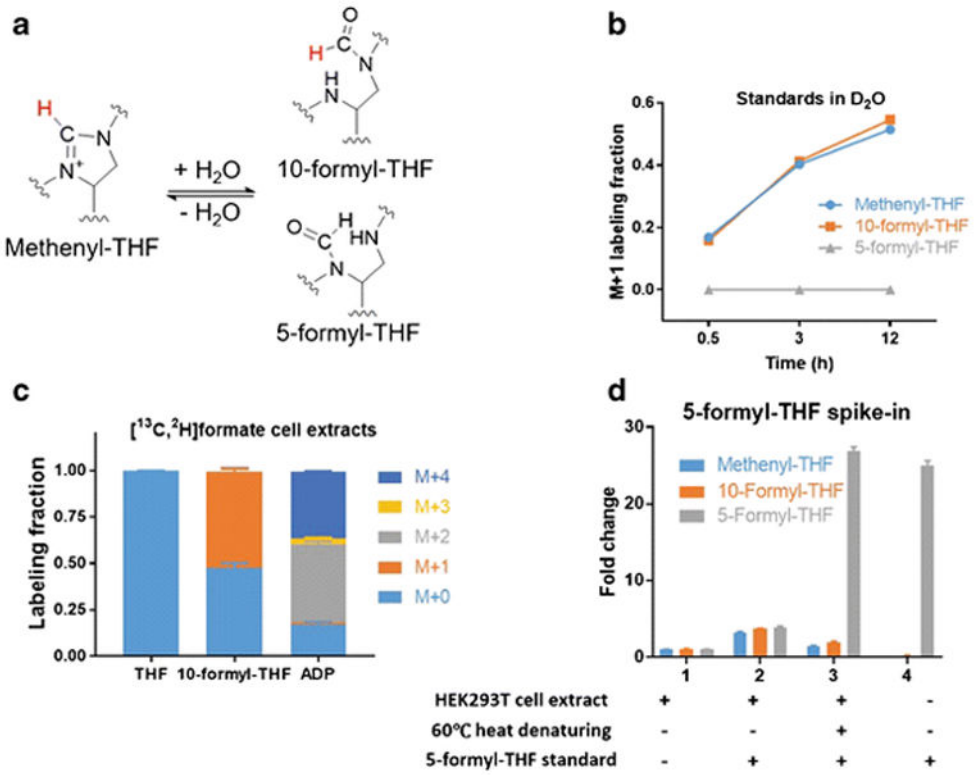


**Figure 3. Residual enzymatic conversion of 5-formyl-THF to methenyl-THF in lysates**

(a) Reaction schematic for methenyl-THF, 10-formyl- and 5-formyl-THF interconversion. The proton highlighted in red can exchange with H2O.

(b) Labeling kinetics of freshly dissolved unlabeled methenyl-THF standard incubated in D2O phosphate buffer (pH 7) at 4°C. To verify that 5-formyl-THF, unlike 10-formyl-THF, does not interconvert with methenyl-THF under these conditions, an identical experiment was performed with 5-formyl-THF standard (Mean ± SD, N = 3).

(c) Folate and metabolite labeling patterns after 24 h incubation of in HEK293T cells with 1 mM [13C,2H]formate in the growth media (Mean ± SD, N ≥ 2).

(d) Conversion of 5-formyl-THF to methenyl-THF in cell extracts. HEK293T cell extracts were prepared as described in method, and optionally heated to 60°C for 5 min after addition (when indicated) of 4 pmol 5-formyl-THF standard (Mean ± SD, N = 3).

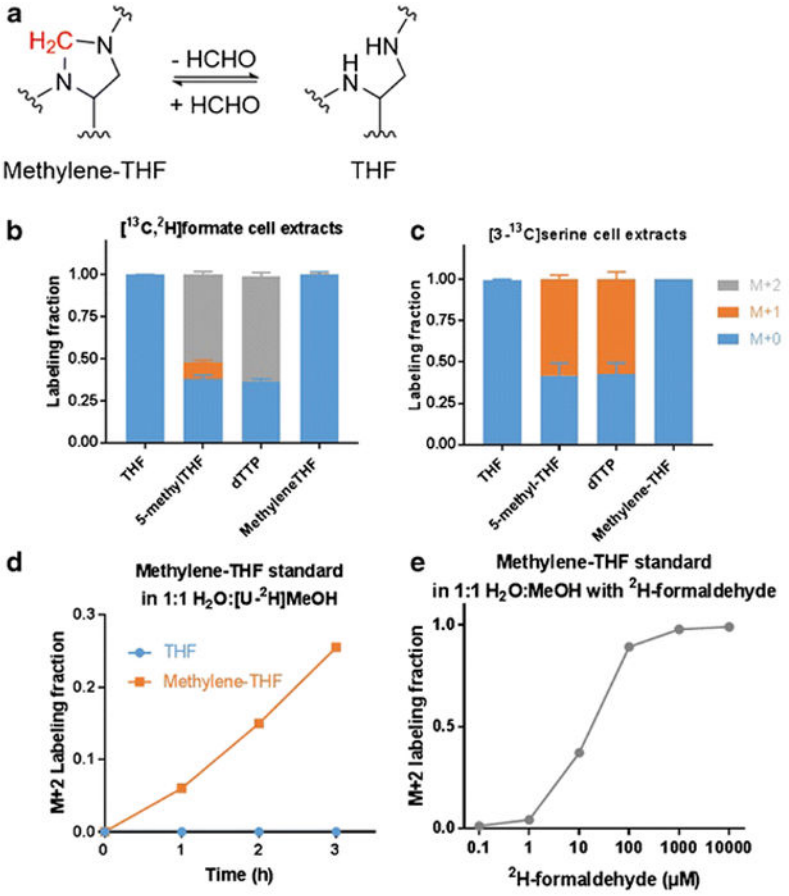


**Figure 4. Methylene-THF's 1C unit exchanges with formaldehyde**

(a) Reaction schematic for THF and methylene-THF interconversion. The methylene group highlighted in red can exchange with formaldehyde.

(b) Labeling patterns in HEK293T cells after 24 h incubation with [3-13C]serine. Note the lack of labeling of methylene-THF, despite labeling of its downstream products, indicative of label loss during the sample preparation process (Mean ± SD, N = 3).

(c) Labeling patterns in HEK293T cells after 24 h incubation with 1 mM [13C,2H]formate (Mean ± SD, N = 3).

(d) Labeling kinetics of freshly dissolved unlabeled THF or methylene-THF standard incubated in 1:1 H2O:[U-2H]MeOH at 4°C.

(e) Labeling pattern of freshly dissolved unlabeled methylene-THF standard incubated at 4°C for 2 h in unlabeled H2O:MeOH with the indicated concentration of deuterated formaldehyde.

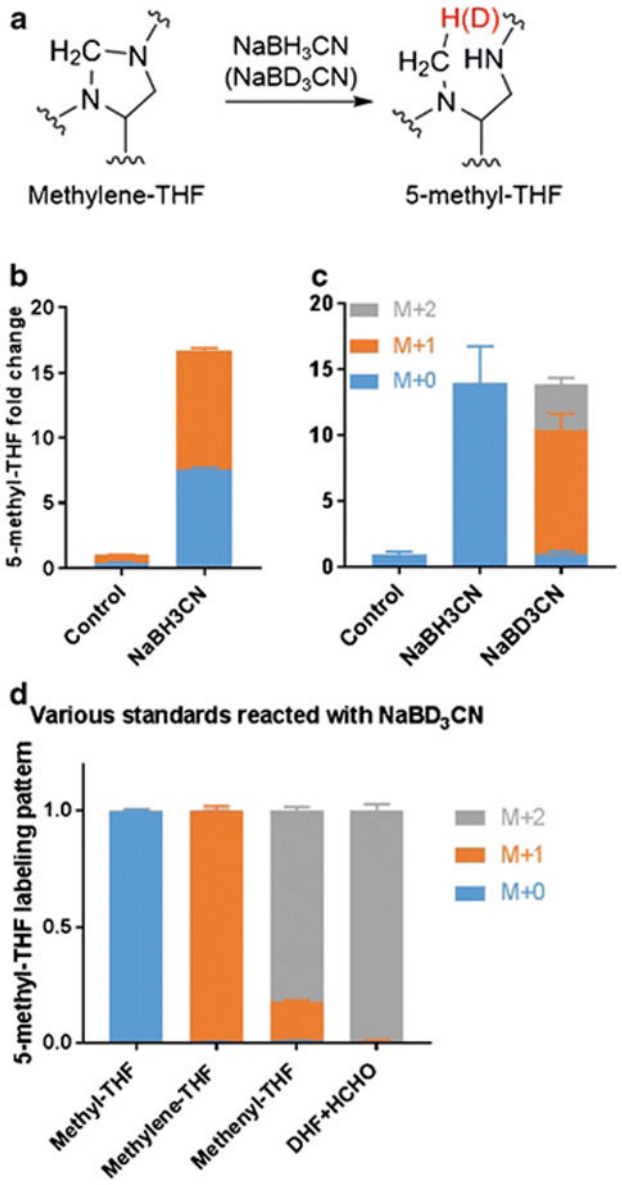


**Figure 5. Quantification of methylene-THF via NaBD3CN reduction**

(a) Reduction of methylene-THF to 5-methyl-THF with NaBH3CN (or NaBD3CN). The hydrogen highlighted in red comes from the reducing reagent.

(b) Change in 5-methyl-THF signal upon NaBH3CN reduction of cell extracts.

(c) Change in 5-methyl-THF signal upon NaBD3CN reduction of cell extracts. Data in (b) and (c) are mean ± SD, N = 3.

(d) 5-methyl-THF labeling after NaBD3CN reduction of the indicated folate standards. DHF + HCHO indicates DHF standard incubated with 0.1% unlabeled formaldehyde (Mean ± SD, N ≥ 2).

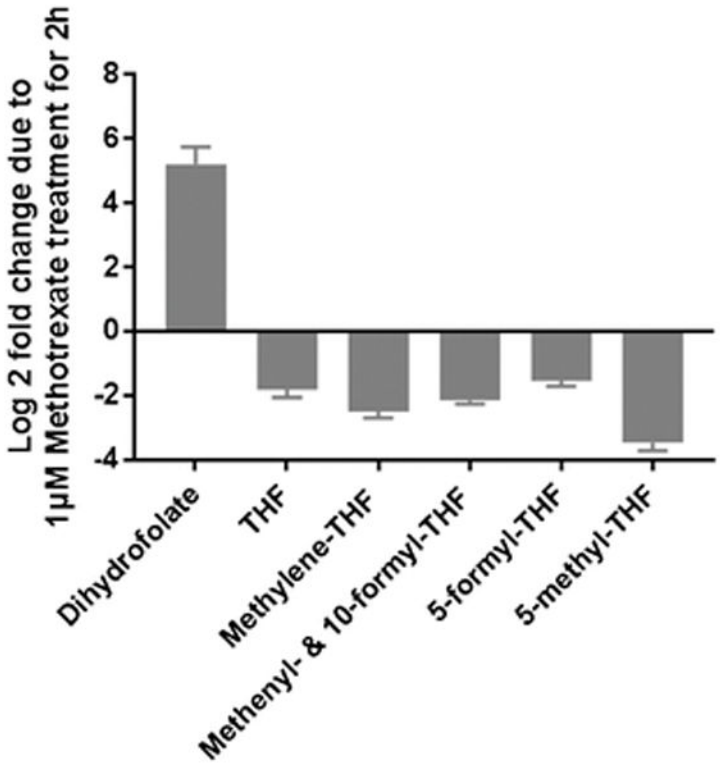


**Figure 6.**

Acute effect of methotrexate on cellular folates. HEK293T cells were incubated with 1 μM methotrexate for 2 h before extraction. Pool sizes are normalized to DMSO-treated control cells (Mean ± SD, N ≥ 3).

**Table 1**

LC-MS method performance for folate standards.

| THF species | Detection limit (nmol/L)[a] | Linear range (nmol/L)[b] | Reproducibility at 100 nmol/L[c] | Retention time (min) |
|---|---|---|---|---|
| THF | 2 | 2–5000 | 2.8% | 9.56 |
| Methylene-THF | 10 | 10–5000 | 2.5% | 9.82 |
| Methenyl-THF | 5 | 5–5000 | 3.2% | 8.09 |
| 5-formyl-THF | 1 | 1–2000 | 2.3% | 9.73 |
| 10-formyl-THF | 2 | 2–2000 | 3.1% | 9.57 |
| 5-methyl-THF | 1 | 1–2000 | 3.2% | 10.02 |

[a]The lowest concentration of standard which generated a signal 5-fold greater than blank.

[b]Range for which R2 >0.99.

[c]Relative standard deviation of 5 replicates.

**Table 2**

Concentration of 5 different THF pools in HEK293T cells, mean ± S.D.

| THF species | Cellular concentration (μmol/L PCV) |
|---|---|
| THF | 1.4±0.6 |
| Methylene-THF | 1.0±0.2 |
| Methenyl-THF + 10-formyl-THF | 1.1±0.1 |
| 5-formyl-THF | 0.19±0.02 |
| 5-methyl-THF | 0.09±0.03 |